

7. Rare-Earth Zirconates ($\text{Ln}_2\text{Zr}_2\text{O}_7$): A Family of Ceramic (Nano) Materials

Melita Menelaou

Department of Chemical Engineering,
Cyprus University of Technology,
3036 Limassol, Cyprus.

7.1 Introduction:

Rare earth (RE) elements (or Lanthanoids) are a group of seventeen chemical elements in the periodic table: namely, fifteen lanthanides (Ln) or 4f elements ($Z = 57-71$), scandium (Sc) ($Z = 21$), and yttrium (Y) ($Z = 39$). The lanthanide series is the following: Lanthanum (La), Cerium (Ce), Praseodymium (Pr), Neodymium (Nd), Promethium (Pm), Samarium (Sm), Europium (Eu), Gadolinium (Gd), Terbium (Tb), Dysprosium (Dy), Holmium (Ho), Erbium (Er), Thulium (Tm), Ytterbium (Yb), and Lutetium (Lu). Scandium and Yttrium exhibit similar chemical properties as the lanthanides and thus they are altogether considered as rare earth elements. The first rare earth element which was discovered was Ytterbite (1787) from Lieutenant Carl Axel Arrhenius. Later, in 1800, Ytterbite was renamed to Gadolinite. Lanthanide chemistry has been extensively studied these last 3 decades, after the scientific community recognized that these elements have unusual physicochemical properties including fluorescent and magnetic properties. The main reason for these features is the presence of the 4f electrons which results in ligand-field effects for the trivalent ions. The electronic configurations of the lanthanides are $5d^16s^2$ for La, $4f^m5d^16s^2$ for Ce ($m = 1$), Gd ($m = 7$), and Lu ($m = 14$), and $4f^n6s^2$ for Pr→Eu ($n = 3-7$), and Dy→Yb ($n = 9-14$), respectively. Divalent lanthanides can therefore have the electronic structure $4f^{n-1}5d^1$, and trivalent lanthanides have a $4f^n$ configuration ($n = 0-14$).

Nowadays, scientists are preparing efficiently lanthanide-based materials for advanced applications; lanthanides are often referred to as “the seeds of technology” – a statement that highlights how important are the lanthanide-based materials for many technological purposes including solar cells, batteries, turbines, and lasers. Some years ago, the scientific community believed that only some of these elements had redox chemistry ($\text{Ce}^{4+}/\text{Ce}^{3+}$ and $\text{Ln}^{3+}/\text{Ln}^{2+}$ where Ln = La, Sm, Eu, and Yb). Nowadays, we know that all elements in this series have redox chemistry. Lanthanides are strong Lewis acids that can coordinate with hard bases (carboxylates) as well as highly electronegative donors (N or O) whilst coordination with water (or other solvents) is also often found.¹

The research community has recently shown an increased interest in a family of ceramic materials often called as rare-earth zirconates (or lanthanide zirconates or lanthanide zirconium oxides). The general formula of these materials is $\text{A}_2\text{B}_2\text{O}_7$ (where A = trivalent lanthanide ion, B = tetravalent transition metal ion such as Zr^{4+} , Ti^{4+} , Mo^{4+});² thus it is transformed to $\text{Ln}_2\text{Zr}_2\text{O}_7$ (or $\text{RE}_2\text{Zr}_2\text{O}_7$).

The increased interest for these materials is because of specific properties that render them excellent candidates for applications in the immobilization of radioactive waste,³ in thermal barrier coatings,⁴ and in photocatalysis.⁵ Rare-earth zirconates crystallize in the cubic structure at room temperature and at ambient pressures. Depending on the ionic radius ratio (RR) among the two metallic ions, $RR = r_{Ln^{3+}} / r_{Zr^{4+}}$, their structure can be stabilized with one of the two following space groups, either *Fd3m* (No. 227), which corresponds to the pyrochlore structure (P) (presence of large lanthanide ion), or *Fm3m* (No. 225) which corresponds to the defect-fluorite structure (F) (presence of small lanthanide ion).²

In particular, when the Ln element varies from Tb to Lu (when Ln = Tb→Lu), in the Ln₂Zr₂O₇ structure where the ionic radius ratio ranges from 1.44 to 1.35, these materials crystallize in a defect-fluorite structure.² Compounds Ln₂Zr₂O₇ (where Ln = La → Gd) with the ionic radius ratio to range from 1.61 to 1.46, then these materials adopt the cubic pyrochlore structure.²

The final annealing temperature can also be a crucial factor for the final structure. Their crystallographic structure contains two different cation sites and two distinct anion sites. Namely, the large trivalent lanthanide ions (Ln³⁺) occupy the eight-fold oxygen coordinated A sites, and the six-fold coordination of the B sites is filled by the smaller tetravalent zirconium ions (Zr⁴⁺) and 1/8th of the oxygen positions is vacant.

Thermally, upon application of pressure and/or chemical doping, pyrochlore structure can transform to the fluorite one. In particular, the 'P' structure can be considered as being derived from the 'F' structure by removing one eighth of the anions in such a way that the vacancies constitute a diamond sublattice (Figure 7.1).⁶

Many of these phases undergo a high-temperature order-disorder (P→F) phase transformation at elevated temperatures (1530–2400 °C),⁷ which has a strong influence on their physicochemical properties. The characteristic peaks that always, make the pyrochlore form diverse from the fluorite phase are (3 3 1) and (5 1 1). Among the rare-earth zirconate pyrochlores, there is a subgroup called defective pyrochlores such as the case of Gd₂Zr₂O₇ which show an incompletely disordered atomic array at ambient condition.

Pyrochlore materials show ionic, electronic, or mixed conductors and unusual magnetic properties. Doping with divalent cations such as Mg²⁺, Ca²⁺, Ba²⁺ and Sr²⁺ at the A site, and/or trivalent cations at the B site, can introduce further oxygen vacancies and increase protonic conductivity.

At high temperature (>1500 °C), Ln₂Zr₂O₇ materials (when Ln = Nd→Gd), undergo an order-disorder transition from a 'P' to a structure 'F' structure. The transition temperature depends on the nature of the rare-earth ion. Thus, lanthanum zirconate (when Ln = La) exists only in the pyrochlore structure, whereas for neodymium, samarium, and gadolinium zirconates, the transition from a pyrochlore to a fluorite structure occurs at 2300, 2000, and 1530 °C, respectively.^{2a} More recent studies however have proven that the lanthanide zirconate with a pyrochlore structure is not stable at high pressure and it undergoes a pressure induced structural transformation to a monoclinic phase (space group *P2₁/c*),⁸ or to a defect cotunnite-type structure (space group *Pnma*).⁹

7.2 Synthetic Methodologies of $\text{Ln}_2\text{Zr}_2\text{O}_7$:

Synthesis is the most important step in solid-state chemistry research and in materials science. Samples may be prepared in various as single crystals, polycrystalline powder, or a thin film. The physicochemical, thermal, and magnetic properties and therefore the applications of such materials depend significantly on the chemical composition, the shape and size of the particles, as well as the morphology.

All these factors are dramatically influenced by the applied synthetic methodology to obtain the rare-earth zirconates. Different wet chemistry approaches have been introduced for the synthesis of rare earth zirconates (Figure 7.2 and 7.3).¹⁰ All wet chemistry methods involve mixing of reactant precursors at the molecular level, thus better compositional homogeneity and stoichiometric control is achieved. The most common synthetic techniques are mentioned below.

7.3 Solid State Synthesis:

Solid-state synthesis (or the ceramic method) is frequently used to form a chemical reaction from solid starting materials (salts, metal oxides, etc) to form a new solid with a well-defined structure. End products include polycrystalline materials, single crystals, glasses, and thin-film materials that are widely used for energy and electronic applications among others.

Modern preparation techniques for solid state are not limited to variations on the ceramic method and many reports exist in the literature to support the technical details during preparation. The general procedure includes mixing of the zirconium source (usually in the form of ZrO_2 or ZrOCl_2) and the lanthanide oxide (Ln_2O_3) powders at high temperature under Ar atmosphere for long period of time (i.e. 10 hours).

The temperature should be in accordance with the nature of the lanthanide ion. The next step is calcination (or sintering) of the obtained powders at high temperatures for long duration of time in order to obtain $\text{Ln}_2\text{Zr}_2\text{O}_7$ ceramic materials.¹¹ Typical characterizations of such materials includes techniques such as XRD and SEM.

7.4 Coprecipitation:

Coprecipitation method is a classical and perhaps the simplest approach for synthesizing materials. The size, morphology, and composition of the as-prepared material can be controlled by a series of experimental parameters, such as the type of precursors, the precursor ratio, the surface ligand (if present), the reaction temperature, and the pH. In a typical coprecipitation method, an aqueous solution of $\text{Ln}(\text{NO}_3)_3 \cdot 6\text{H}_2\text{O}$ and $\text{ZrOCl}_2 \cdot 8\text{H}_2\text{O}$ in presence of ammonia ($\text{pH} > 8$) lead to the formation of precipitation of metal ions in the form of hydroxide. Further, calcination is required at high temperature and for long duration of time in order to finally prepare the $\text{Ln}_2\text{Zr}_2\text{O}_7$ structures.¹² Through coprecipitation homogeneous materials with high purity can be obtained. In case of large grain-sized powders, an additional milling step may be necessary.

7.5 Hydrothermal/Solvothermal:

During the hydrothermal/solvothermal synthesis, the precursors are dissolved in a suitable solvent, and then transferred to an autoclave or a sealed glass tube. Usually the pressure is controlled by the gas law [$P = f(T)$], even though the pressure of some reactors can be controlled.

The pH adjustment (typically $\text{pH} > 7$) is achieved through the addition of a base agent such as ammonium hydroxide or sodium hydroxide. The hydrothermal/solvothermal synthesis is the only method that requires lower reaction temperature (typically 200-400 °C) compared to the above-mentioned methods and uses water as solvent or other common organic solvents.

For example, Hongming and Danqing prepared lanthanum zirconates by hydrothermal method using lanthanum nitrate, and zirconium nitrate salts, as well as NaOH to adjust the pH at 11. The hydrothermal reaction was completed at 200° C in 1 hour.¹³

7.6 Sol-Gel:

Sol-gel is another technique to synthesize of ceramic materials such as metal oxides, nitrides, and carbides. This is a simple, low-cost technique and environmentally friendly technique where Ln₂Zr₂O₇ materials with high sintering capacity can be synthesized under low reaction temperatures with good composition control, and high purity level. Very well-known porous structured materials such as zirconia or yttria-stabilized zirconia can be prepared under this technique.

The reaction mainly occurs by hydrolysis and condensation of a precursor resulting in the formation of a sol that, after a series of chemical reactions and/or mild thermal treatments, turns into a gel. The final material is obtained after calcination.¹⁴

7.7 Other Techniques:

7.7.1 Combustion:

Combustion method involves a simple reaction between fuel agents such as citric acid, glycine and hydrazine and metal precursors (oxidants). For example, lanthanum zirconate was synthesized by Matovic et al. by dissolving first La(NO₃)₃·6H₂O and zirconium chloride in glycine; then the prepared solution was heat-treated at 950 °C for 120 minutes and finally sintered at 1600 °C for 4 hours. This method helps to produce porous pyrochlore powders with high efficiency and uniform morphology.¹⁵

7.7.2 Floating Zone:

In the floating zone growth, the molten zone is kept between two vertical solid rods and a single crystal is grown by dipping a seed crystal into one end of the zone and translating the molten zone toward the feed stock.

The main advantage of this technique is the absence of the container, which precludes a contamination by the crucible material and the generation of crystal defects caused by the interaction between the growing crystal and the container.¹⁶

7.8 Application of Ln₂Zr₂O₇ Ceramic Nanomaterials – Thermal Barrier Coatings:

Complex oxides such as the rare-earth zirconate ceramic materials in the ‘F’ and/or ‘P’ structure display a variety of interesting and promising physical, chemical, thermal and magnetic properties which render them excellent candidates in applications such as photocatalysis, magnetism, solid electrolytes in high-temperature fuel cells and thermal barrier coatings, among others.

The performance of these materials in applications largely depends on their crystallinity, size, shape and surface structure. In addition, these ceramic materials display high thermal stability, chemical resistance, high thermal expansion coefficients, high melting points, low thermal conductivities, great ionic conductivity, and high sintering rate among others.

Nowadays, there is an increasing demand in energy efficiency and power generation and that is why the development of new technologies and advanced materials using environmentally friendly approaches and cost-effective production systems, appears mandatory.

Any significant technological step towards this direction, is immediately associated with the energy goals of the EU; namely, this is one out of five priorities based on the new EU energy strategy.¹⁷ High-temperature gas-turbine engines are nowadays widely used to generate a huge amount of energy (land-based turbines) and transport (aerospace gas-turbines).

One of the challenges for the industrial and gas-turbine engines for today's scientists, is to unravel the technological know-how in order to reduce both fuel consumption and pollutants emissions.¹⁸ Another significant challenge is to increase the operating temperature of the engines to a maximum temperature during operation and, at the same time, guarantee that the metallic parts of the turbines are not overheated.¹⁹

One suggestion on addressing these scientific and technological challenges is based on the optimization of the engine design; modelling and prediction tools are necessary to estimate parameters such as the turbulent flow, combustion chamber flow, position of internal cooling channels in lines and blades, and heat transfer.

Another suggestion is dedicated on the materials which cover both the combustion chamber and blades as Thermal Barrier Coatings (TBCs).²⁰ TBCs are the most effective and advanced ceramic systems for the protection and isolation of the hot section parts of turbine engines that allow higher combustion temperatures and thus, they can improve the efficiency of gas-turbine engines.²¹

Typical TBC structures (100 μm to 1 mm in thickness) for gas-turbine engines comprise of a bond-coat (typically made of MCrAlY; where M=Ni, Co, or a mixture of Co/Ni), a thermally grown oxide (TGO), and a ceramic top-coat; a TBC being deposited onto a metallic substrate (Ni-based superalloy). In some cases, the bond-coat may also consist of more than one layer, each of different chemical/phase composition.²² Currently, yttria-stabilized zirconia (7-8% of Y₂O₃-ZrO₂; YSZ) is the principal ceramic material used as top-coat layer for TBCs in high-temperature sections of aircraft gas-turbine engines.²³

This is due to the desirable properties of YSZ. Namely YSZ has a high melting point (~ 2700 °C), one of the lowest thermal conductivity ($\sim 2.3 \text{ Wm}^{-1}\text{K}^{-1}$ at ~ 1000 °C), a high thermal-expansion coefficient (CTE) ($\sim 11.10 \times 10^{-6} \text{ }^\circ\text{C}^{-1}$), and good thermal and chemical stability.²⁴

However, YSZ-based TBCs (YSZ-TBCs) which are exceptional materials face severe limitations since the expectations regarding the TBC temperature capability continue to increase: the maximum surface temperature for conventional YSZ-TBCs is limited up to 1200 °C. Above 1200 °C, changes are observed in phase composition, microstructure and properties, which altogether are associated with high thermally-induced stresses. We can say that the existing YSZ-TBCs have reached the limits in terms of temperature capability.

In addition, YSZ-TBCs are subjected to a variety of aggressive environments leading to coating degradation due to ingestion and infiltration of calcia-magnesia-alumino-silicate (CMAS) environmental attack.²⁵ CMAS resistance can be achieved by adding one or more layers. Hence, there is the urgent need to develop the next generation of advanced Thermal and Environmental Barrier Coatings (TEBCs) using environmentally friendly and inexpensive deposition techniques which can combine desirable properties of YSZ and reach today's demands for higher temperature capabilities, high performance and significantly reduced degradation under severely aggressive environments. Among various requirements, these systems must have low thermal conductivity ($0.5\text{-}1 \text{ Wm}^{-1}\text{K}^{-1}$), phase stability at high temperatures, CTE close to that of the metallic substrate ($>9 \times 10^{-6} \text{ }^\circ\text{C}^{-1}$), chemical compatibility with the underlying YSZ and appropriate CMAS resistance. Advanced ceramic materials can play the key role. The replacement of the metallic components of the existing systems seems less promising.

The development of advanced ceramic systems in a multilayer architecture, seems to be the most promising strategy to achieve the full potential of advanced ceramics.

Over the last decade, strategies have been proposed to replace YSZ to overcome the limitations of conventional TBCs.^{24b} However, due to the specificity and selectivity of YSZ for TBCs, all strategies had limited success.

Thus, a new opportunity arises now to discover new materials in the form of multilayer TBCs. For this purpose, rare-earth zirconates of pyrochlore and fluorite structure,²⁵ can be promising candidates. A typical example of such ceramic materials is lanthanum zirconate (LZ) (pyrochlore structure of La₂Zr₂O₇; Ln=La) and its properties (i.e. lower thermal conductivity than YSZ; $1.5\text{-}1.8 \text{ Wm}^{-1}\text{K}^{-1}$ at ~ 1000 °C, no phase transformation, CMAS resistance)²⁶ suggest that this material has many advantages when compared to YSZ.

Thus, LZ can act as top-coat layer(s) (LZ_x; x refers to a single layer or more layers) in multilayered architecture. The coating architecture and properties depend significantly on the ceramic materials used for the coatings.

Multilayer TBCs which comprise of advanced LZ_x top-coat layers and the currently prominent material YSZ as a middle layer, can provide a promising multilayer TBC candidate system (MCrAlY-YSZ-LZ_x) suitable to overcome the limitations of the conventional TBCs (MCrAlY-YSZ).

7.9 Conclusion:

Rare earth zirconate ceramic nanomaterials represent a class of materials with interesting physicochemical, magnetic, thermal, and optic properties. Altogether they lead to potential technological applications spanning from photocatalysis, magnetism, and nuclear waste storage, to solid electrolytes in high-temperature fuel cells and thermal barrier coatings.

This chapter describes the basic physicochemical features of these materials as well as the most common synthetic methodologies to obtain them. The last section of this chapter covers one significant potential application of the rare-earth zirconates which is the thermal barrier coatings.

Figures and Figure Captions:

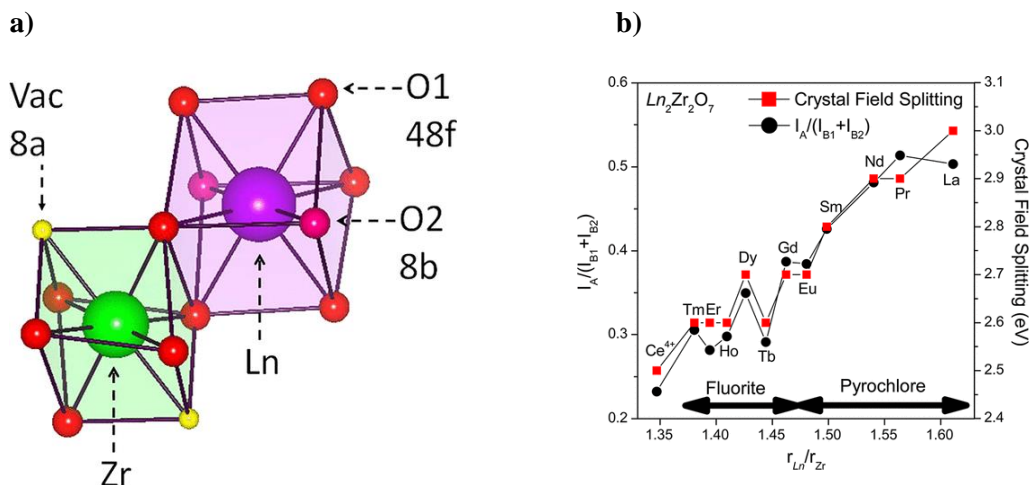


Figure 7.1: (a) Representation of the pyrochlore structure showing the relationship to the fluorite structure. In the fluorite the 8a sites are fully occupied, and (b) Plots of the crystal field splitting (ΔE) and the intensity ratio of features A and B ($I_A / (I_{B1} + I_{B2})$) as a function of r_{Ln} / r_{Zr} . Peak intensities are taken as the area of the peaks. (Reproduced from Ref. [6] with permission of the American Chemical Society).

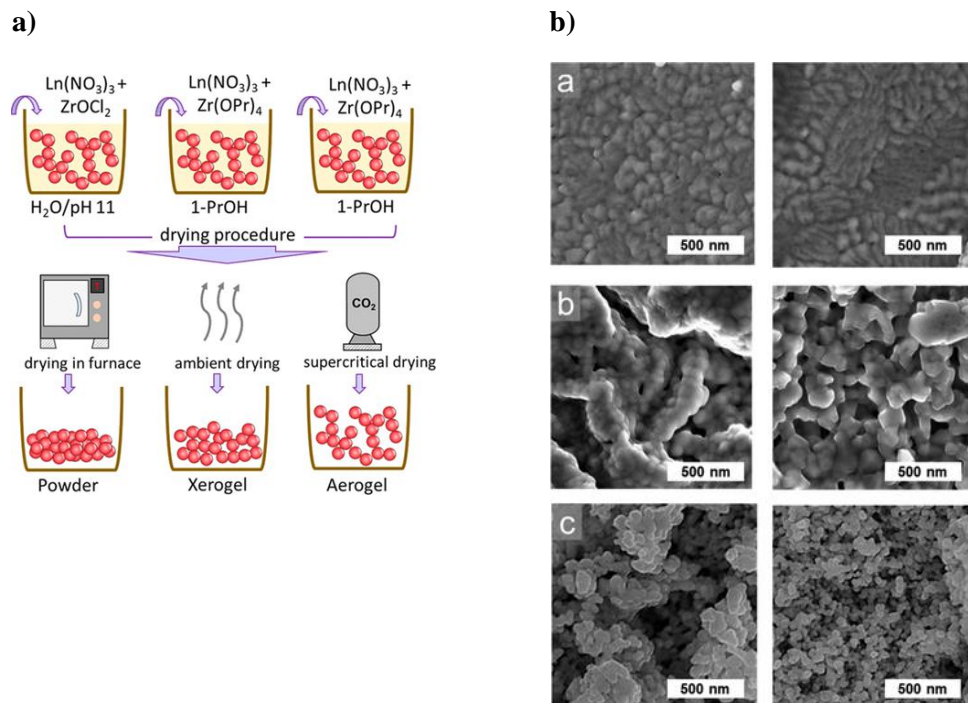


Figure 7.2: (a) Schematic representation of $\text{Ln}_2\text{Zr}_2\text{O}_7$ nanostructured materials prepared using different drying protocol and (b) Scanning electron microscopy: surface morphology of the calcined $\text{La}_2\text{Zr}_2\text{O}_7$ and $\text{Gd}_2\text{Zr}_2\text{O}_7$ (i) powders, (ii) xerogels, and (iii) aerogels at $1000^\circ\text{C}/5\text{ h}$. (Reproduced from Ref. [10a] with permission of the American Chemical Society).

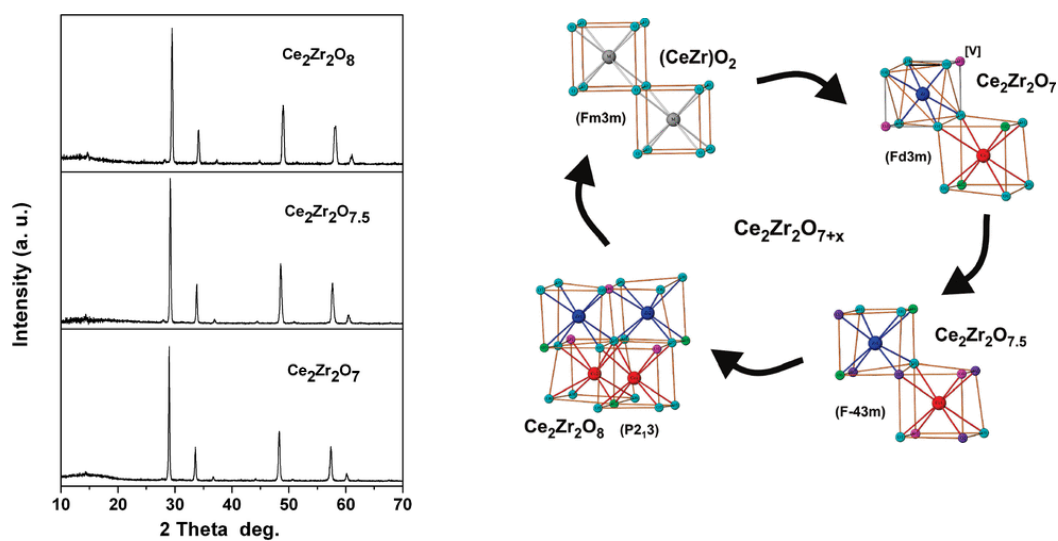


Figure 7.3: (a) Powder XRD patterns and (b) structural transformations in $\text{Ce}_2\text{Zr}_2\text{O}_7$, $\text{Ce}_2\text{Zr}_2\text{O}_{7.5}$, and $\text{Ce}_2\text{Zr}_2\text{O}_8$, respectively. (Reproduced from Ref. [10b] with permission of the American Chemical Society).

7.10 References:

1. For example, see: (a) N. C. Martinez-Gomez, et al. *Inorg. Chem.* 2016, 55, 10083–10089; (b) S. Nief, *Handbook on the Physics and Chemistry of Rare Earths*; Elsevier Science BV: Amsterdam, the Netherlands, 2010; (c) M. R. MacDonald, et al. *J. Am. Chem. Soc.* 2013, 135, 9857–9868.
2. For example, see: (a) M.A. Subramanian, et al. *Progress in Solid State Chemistry*, 1983, 15, 55–143; (b) B. P. Mandal and A. K. Tyagi. *J. Alloys & Comps.* 2007, 437, 260-263.
3. W.J. Weber, R.C. Ewing, *Science*, 2000, 289, 2051-2052.
4. X. Cao, F. Tietz, *J. Amer. Cer. Soc.* 2000, 83, 2023-2028.
5. S. Zinatloo-Ajabshir, et al. *Mater. Lett.* 2016, 180, 27-30.
6. P. E. R. Blanchard, et al. *Inorg. Chem.* 2012, 51, 13237-13244.
7. J M. P. Saradhi, et al. *RSC Advances* 2012, 2, 3328-3334.
8. S. Surblé; *Phys. Chem. Minerals* 2010, 37, 761-767.
9. J. Rodríguez-Carvajal, *Physica B* 1993, 192, 55-69.
10. (a) J. Torres-Rodriguez, et al. *Inorg. Chem.* 2019, 58, 14467-14477; (b) S. Nagabhusan Achary, et al. *Chem. Mater.* 2009, 21, 5848-5859.
11. For example, see: (a) W. Duarte, et al. *Journal of Materials Science* 2015, 50, 463-475; (b) J. Zhang, *Surface and Coatings Technology* 2017, 323, 18-29.
12. For example, see: (a) Z.-G. Liu, *Ceramics International* 2009, 35, 791-796; (b) X. Cao, *Journal of the American Ceramic Society* 2000, 83, 2023-2028.
13. For example, see: (a) Z. Hongming, and Y. Danqing. *Journal of Rare Earths* 2008, 26, 770-774; (b) A. Matsuda, et al. *Catalysts*, 2000, 10, 1392 (20 pages).
14. For example, see: (a) J.M. Sohn, et al. *Catal. Today* 2003, 83, 289-297; (b) M. Uno, et al. *J. Alloys Compd.* 2006, 420, 291-297.
15. For example, see: (a) B. Matovic, et al. *Journal of the European Ceramic Society* 2020, 40, 2652-2657; (b) W. Li, et al. *Journal of the European Ceramic Society* 2020, 40, 1665-1670.
16. For example, see: (a) M. Ciomaga Hatnean, et al. *Journal of Crystal Growth* 2015, 418, 1-6; (b) K. Kimura, et al. *Nat. Commun.* 2013, 4, 1934 (6 pages).
17. European Commission's communication 'Energy 2020-A strategy for competitive, sustainable and secure energy' November, 2010.
18. P. Ramu and C.G. Saravanan, *Energ. Fuel* 2009, 23, 653-656.
19. N.P. Padture, *Nat. Mater.* 2016, 15, 804-809.
20. T.M. Pollock, *Nat. Mater.* 2016, 15, 809-815.
21. a) A. Marshall Stoneham and J.H. Harding, *Nat. Mater.* 2003, 2, 77-83; b) K. Knipe, et al. *Nat. Commun.* 2014, 5, 4559 (pp 1-7).
22. N.P. Padture, et al. *Science* 2002, 298, 280-284.
23. (a) D. R. Clarke, et al. *MRS Bull.* 2012, 37, 891-898; (b) R. Vassen, et al. *J. Am. Ceram. Soc.* 2000, 83, 2023-2028.
24. (a) E. Bakan and R. Vaßen, *J. Therm. Spray Tech* 2017, 26, 992-1010; (b) J. H. Perepezko, et al. *J. Therm. Spray Tech* 2017, 26, 929-940.
25. V. Viswanathan, et al. *J. Am. Ceram. Soc.* 2015, 98, 1769-1777.
26. (a) S. Zhang, et al. *Sci. Rep.* 2017, 7, 6399 (pp 1-13); (b) J. Zhang, et al. *Surf. Coat. Tech.* 2017, 323, 18-29; (c) U. Schulz and W. Braue, *Surf. Coat. Tech.* 2013, 235, 165-173.